RAPID REPORT

Muscarinic receptor activation tunes mouse stratum oriens interneurones to amplify spike reliability

J. Josh Lawrence, Zachary M. Grinspan, Jeffrey M. Statland and Chris J. McBain

Laboratory of Cellular and Synaptic Neurophysiology, National Institute of Child Health and Human Development, National Institutes of Health, Bethesda, MD, USA

Cholinergic activation of hippocampal targets can initiate and sustain network oscillations *in vivo* and *in vitro*, yet the impact of cholinergic modulation on the oscillatory properties of interneurones remains virtually unexplored. Using whole cell current clamp recordings in acute hippocampal slices, we investigated the influence of muscarinic receptor (mAChR) activation on the oscillatory properties of CA1 stratum oriens (SO) interneurones *in vitro*. In response to suprathreshold oscillatory input, mAChR activation increased spike reliability and precision, and extended the bandwidth that interneurone firing phase-locked. These suprathreshold effects were largest at theta frequencies, indicating that mAChR activation tunes active conductances to enhance firing reliability and precision to theta frequency input. Muscarinic tuning of the intrinsic oscillatory properties of interneurones is a novel mechanism that may be crucial for the genesis of the theta rhythm.

(Received 7 December 2005; accepted after revision 19 January 2006; first published online 26 January 2006)
Corresponding author J. Lawrence: Laboratory on Cellular and Synaptic Neurophysiology, Building 35, Rm 3C907, NICHD-LCSN, Bethesda, MD 20892, USA. Email: lawrenjo@mail.nih.gov

Theta oscillations, sustained through reciprocal synaptic interactions between interneurones and pyramidal cells, are thought to be the primary means by which neuronal assemblies bind together distinct aspects of spatial experience (Lisman & Idiart, 1995; Buzsaki, 2002). Recent evidence indicates that morphologically distinct subclasses of interneurones fire at different phases of the theta cycle, thereby making precise contributions to network oscillations (Klausberger *et al.* 2004; Somogyi & Klausberger, 2005). Interneurone-specific differences in action potential (AP) timing during network oscillations arise not only from the nature of their reciprocal connectivity but also in how incoming synaptic inputs are transduced to neuronal outputs (Whittington & Traub, 2003; Gloveli *et al.* 2005). Moreover, interneurone types can exhibit different frequency preferences of AP output even when driven by a common input frequency (Pike *et al.* 2000; Whittington & Traub, 2003; Gloveli *et al.* 2005). This frequency preference arises from interneurone-specific differences in both passive properties and the complement of voltage-gated channels (Pike *et al.* 2000; Schreiber *et al.* 2004).

In vivo studies have demonstrated an important role of cholinergic transmission in the amplification of theta rhymicity (Lee *et al.* 1994). Although *in vitro* models of mAChR-induced network oscillations reveal complex changes in the pattern of synaptic input onto individual interneurones (McMahon *et al.* 1998; Fellous & Sejnowski, 2000; Reich *et al.* 2005), postsynaptic effects of mAChR activation also alter interneuronal output properties (McQuiston & Madison, 1999*b*; Cobb & Davies, 2005; Lawrence *et al.* 2006). For example, horizontally orientated SO interneurones exhibit intrinsic resonance and spike transfer frequency preference in the theta range (5–12 Hz; Pike *et al.* 2000) but it is not clear how mAChR activation influences the oscillatory properties of these cells.

Although a large number of horizontal cell types exist within SO (Maccaferri, 2005), most depolarize upon mAChR activation (McQuiston & Madison, 1999*a*; Lawrence *et al.* 2006). We recently determined that the vast majority of cells with this depolarizing phenotype are the so-called O-LM interneurones (Lawrence *et al.* 2006), named because their axons ramify on the distal dendrites of CA1 pyramidal cells in stratum lacunosum moleculare (LM; Fig. 1*A*; McBain *et al.* 1994). O-LM cells exhibit a prominent M_1/M_3-mediated afterdepolarization (ADP) that can promote sustained firing (Fig. 1*B*; Lawrence *et al.* 2006). Here, we determine how oscillatory activity is impacted by mAChR activation in these cells. We demonstrate that mAChR activation increases firing

J. J. Lawrence and Z. M. Grinspan contributed equally to this work.

© 2006 The Authors. Journal compilation © 2006 The Physiological Society DOI: 10.1113/jphysiol.2005.103218

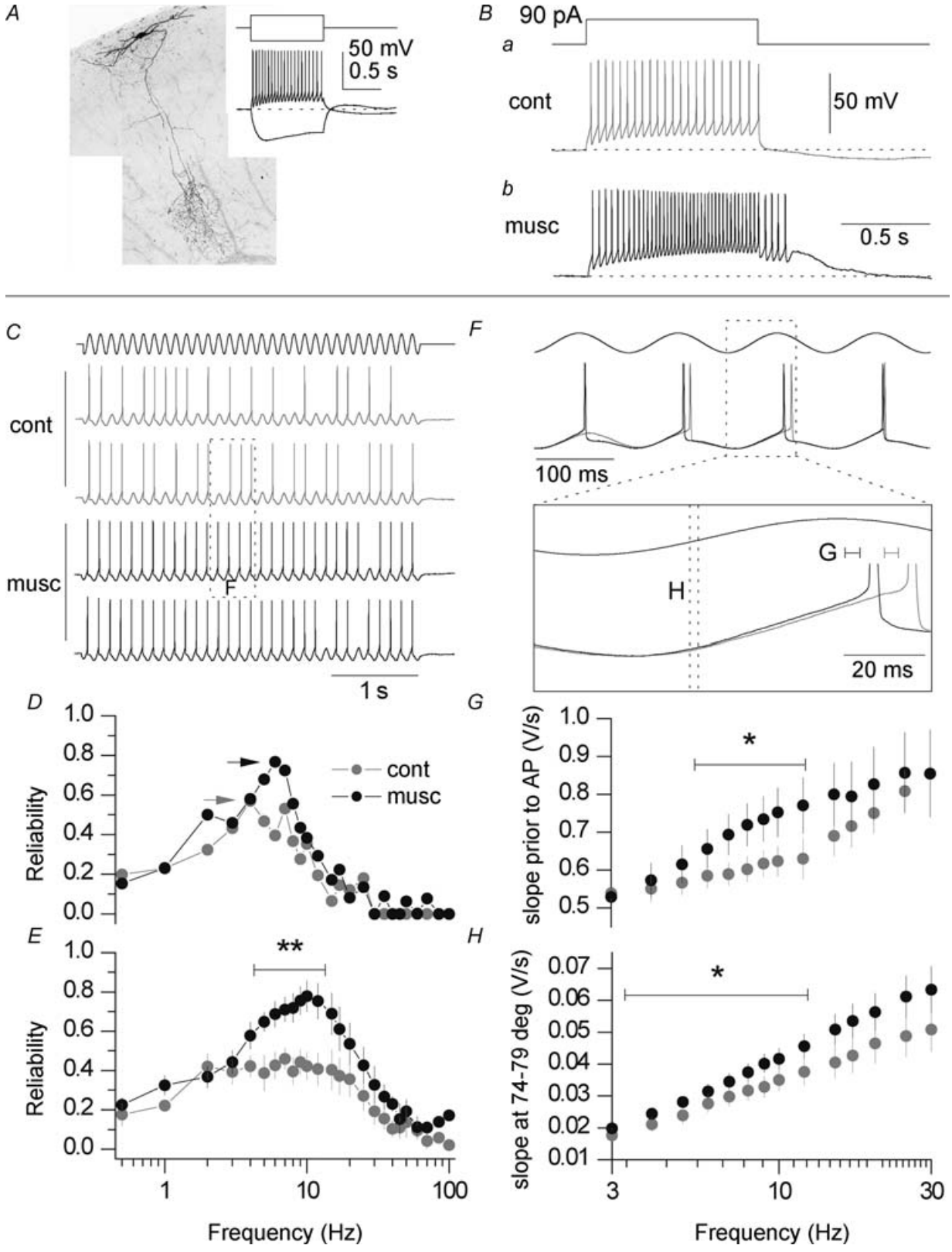

Figure 1. mAChR activation increases firing reliability at theta frequencies
A, O-LM cell and (inset) voltage response to a 1 s, ± 90 pA current step from −60 mV. *B*, voltage response of O-LM cell in *A* in control (*a*) and in the presence of 10 μM muscarine (*b*). *C*–*G*, sinusoidal currents at frequencies 0.5–100 Hz were applied in control (grey) and after application of 10 μM muscarine (black). Bias current was applied such that the cell was maintained at a similar voltage just below threshold in all conditions. *C*, in response

© 2006 The Authors. Journal compilation © 2006 The Physiological Society

reliability and sharpens firing precision to theta frequency input, thereby tuning interneurones to amplify theta oscillations.

Methods

Hippocampal slice preparation and electrophysiological recording were performed as previously described (Lawrence *et al.* 2006). All procedures were carried out according to NIH guidelines. Briefly, 14- to 21-day-old 129J1(50%) × CF1(50%) mice were decapitated under isoflurane anaesthesia and the brains were dissected in ice-cold saline containing (mM): 87 NaCl, 2.5 KCl, 1.25 NaH_2PO_4, 25 $NaHCO_3$, 25 glucose, 75 sucrose, 7 $MgCl_2$, 0.5 $CaCl_2$ saturated with carbogen (95% O_2, 5% CO_2), pH 7.4. Transverse hippocampal slices (300 μm) were cut on a vibratome (Leica) and placed in warm (36°C), continuously oxygenated saline for at least 30 min before use. Interneurones with fusiform cell bodies and horizontal dendrites within SO were visually identified (Infrapatch; Luigs and Neumann) and superfused at a rate of 1–2 ml min^{-1} under carbogen pressure at room temperature (~22°C). Only cells that depolarized, that were clearly excited upon mAChR activation, and that displayed electrophysiological properties characteristic of O-LM interneurones (i.e. sag upon hyperpolarization) were included in the study (Lawrence *et al.* 2006); cells that initially hyperpolarized upon mAChR activation, indicating a different subclass of SO interneurone (Lawrence *et al.* 2006), were not included. The extracellular solution contained (mM): 130 NaCl, 3.5 KCl, 1.25 NaH_2PO_4, 25 $NaHCO_3$, 10 glucose, 2 $MgCl_2$, 2 $CaCl_2$, saturated with carbogen. NMDA, AMPA and $GABA_A$ responses were blocked with DL-APV (100 μM), DNQX (25 μM) and gabazine (5 μM). mAChRs were activated via bath application of 10 μM muscarine. Pipette resistances ranged from 2.5 to 4.5 MΩ when filled with (mM): 135 potassium gluconate, 10 Hepes, 0.1 EGTA, 2 Na_2ATP, 0.3 Na_2GTP, 20 KCl. Recordings were performed with an Axoclamp 200B or Multiclamp 700A amplifier (Molecular Devices, Union City, CA, USA), filtered at 3 kHz (Bessel filter, Frequency Devices, Haverhill, MA, USA), and digitized at 10–20 kHz (Digidata 1320A and pCLAMP Software, Molecular Devices).

Input current protocols and analysis programs were written in Axograph 4.7 (Molecular Devices) by the authors. In Figs 1–3, firing threshold was found empirically by injecting enough bias current to induce a series of APs. The bias current was then reduced until APs were no longer observed. This starting voltage was noted as $V_{baseline}$, and the bias current was adjusted throughout the experiment such that the cell was maintained at $V_{baseline}$ at the beginning of all trials in all conditions. Sinusoidal protocols were repeated 2–5 times in each condition. Due to the influence of voltage level on action potential initiation, trials in which $V_{baseline}$ varied by more than 1–2 mV from the original $V_{baseline}$ value were excluded from the analysis. Moreover, except in Fig. 4, $V_{baseline}$ was within a voltage range such that the ADP was tonically active. This permitted stability in voltage level throughout sinusoidal stimulation, as measured by the negligible average voltage difference in the first and last seconds of the sinusoidal stimulation (-0.046 ± 0.04 mV difference, $n = 8$, $P = 0.30$). Data are presented as means ± S.E.M.

Biocytin (0.2%) was added for *post hoc* morphological identification of each recorded cell. Only cells positively identified as interneurones with somata located in SO were included in the study. Cells were imaged *post hoc* as previously described (Lawrence *et al.* 2006).

Results

Muscarine increases action potential reliability to oscillatory input

O-LM interneurones are participants in oscillatory activity *in vivo* (Cobb *et al.* 1995; Klausberger *et al.* 2003). To investigate how postsynaptic mAChR activation impacts on the intrinsic oscillatory properties of these interneurones, we introduced sinusoidal current injections into these cells across a range of input

to an 8-Hz sinusoidal current injection (4 s, 120 pA peak to peak), the cell fired more regularly in the presence of 10 μM muscarine than in control. *D*, plot of AP reliability *versus* frequency of sinusoidal current for cell in *C* before (●) and after application of 10 μM muscarine (●) shows this cell was maximally reliable (0.57) at 4 Hz in control (grey arrow) and maximally reliable (0.76) at 6 Hz in 10 μM muscarine (black arrow). *E*, plot of AP reliability *versus* frequency for a population of 8 cells (excluding 1 cell, which was done at select frequencies) shows that mAChR activation significantly increased ($P < 0.05$) reliability at each frequency between 5 and 12 Hz ($P > 0.05$ at frequencies < 5 Hz and > 12 Hz). $^{**}P = 6 \times 10^{-5}$, averaging across 5–12 Hz. *F*, overlay of traces from dotted box in *C*, illustrating that mAChR activation induced phase shift. *F*, lower, overlay of traces from dotted box in the above panel, illustrating that mAChR activation was associated with an increased slope (d*V*/d*t*) on the upswing of the sinusoidal cycle. *G*, plot of slope prior to the AP *versus* frequency, as measured in a 3-ms window 2 ms prior to the onset of the AP in control (*F*, grey bar) and in the presence of 10 μM muscarine (*F*, black bar). *Slope significantly increased ($P < 0.05$) at each frequency between 6 and 11 Hz. *H*, plot of slope *versus* frequency with slope measured at a fixed point in the sinusoidal cycle (in a 74–79 degree window; between dotted lines in *F*); *slope significantly increased ($P < 0.05$) at each frequency between 4 and 12 Hz.

© 2006 The Authors. Journal compilation © 2006 The Physiological Society

frequencies in the presence of blockers of synaptic transmission. Although sinusoidal stimulation only grossly approximates rhythmic IPSP/EPSP barrages occurring during *in vivo* oscillations, sinusoidal stimulation has several advantages over synaptically evoked oscillatory input: it allows fine control over the amplitude, frequency and regularity of the input current, as well as the initial membrane potential of the cell (Garcia-Munoz *et al.* 1993; Leung & Yu, 1998; Pike *et al.* 2000).

To determine whether mAChR activation increases AP reliability, sinusoidal currents were introduced into SO interneurones under control conditions and in the presence of 10 μM muscarine. Under these conditions, mAChR activation induced increased firing (Fig. 1*C*). To quantify how well the cell reproduced the same output with repeated trials of the same stimuli, we used a reliability statistic (Schreiber *et al.* 2003; see also Supplemental material Appendix) that is sensitive both to changes in AP presence and timing (Supplemental material Fig. 1). A representative cell is illustrated in Fig. 1*D*. In control conditions, a peak in reliability occurred at approximately 5 Hz, consistent with the

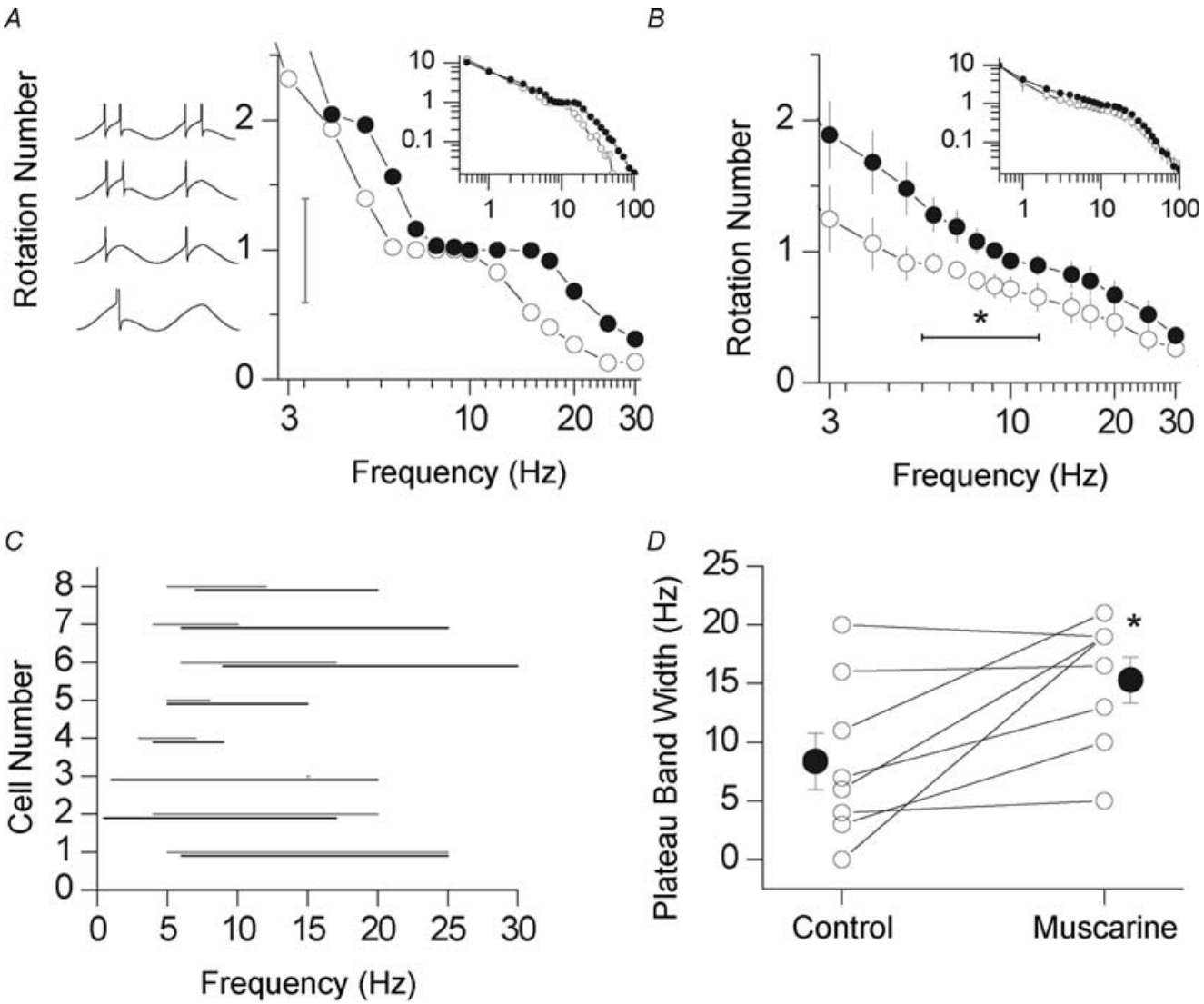

Figure 2. mAChR activation extends the frequency band of 1 : 1 phase locking
A, inset, in a representative cell, rotation number (average spikes per cycle; R#) gradually declines from 12.5 at 0.5 Hz to 0 at 100 Hz in control (○), and 10.7 at 0.5 Hz to 0.016 at 100 Hz after application of 10 μM muscarine (●). *A*, plot of R# *versus* frequency shows that the cell fires approximately every cycle (R# = 1) from 5 to 12 Hz in control (width = 7 Hz) and from 7 to 17 Hz after application of 10 μM muscarine (width = 10 Hz). *B*, inset, mAChR activation increases the average R# in the theta band from 0.79 ± 0.07 (open symbols) to 1.11 ± 0.08 (filled symbols; $n = 9$, $P = 0.007$). *C*, representative cells for frequency bands at which R# is 1 ± 0.4 (vertical grey bar in A) in control and 10 μM muscarine (black bars). *D*, averaging across cells shows this bandwidth is significantly wider after application of 10 μM muscarine (8.4 ± 2.4 *versus* 15.3 ± 2.0 Hz; $P < 0.05$).

© 2006 The Authors. Journal compilation © 2006 The Physiological Society

frequency preference for these cells (Pike *et al.* 2000). Maximum reliability increased after application of 10 μM muscarine, from 0.57 at 4 Hz (grey arrow) to 0.76 at 6 Hz (black arrow). In a population of 9 cells, muscarine increased peak reliability (from 0.69 ± 0.04 to 0.86 ± 0.04, $P = 0.002$) without changing the frequency preference (Fig. 1*E*; 9.3 ± 2.0 *versus* 10.1 ± 1.7 Hz, $P = 0.62$, $n = 9$). The mAChR-induced increase in reliability was largest when averaged across theta frequencies (5–12 Hz, Fig. 1*E*; from 0.45 ± 0.05 to 0.72 ± 0.04, $P = 6 \times 10^{-5}$).

We hypothesized that increased reliability may occur by increasing the slope during the upswing of the sinusoidal cycle, which can effectively lower threshold for AP initiation (Azouz & Gray, 2000). To test this hypothesis, we measured the slope (dV/dt) of the voltage response in a 3-ms window just prior to AP initiation (Fig. 1*F*, bars). mAChR activation increased the slope during the upswing of the cycle (Fig. 1*F*). This increase was statistically significant when averaged over the theta range (Fig. 1*G*, and 0.60 ± 0.03 to 0.71 ± 0.05 V s^{-1}, $n = 8$, $P = 0.009$). To control for timing of the AP within the cycle, we also measured the slope at a fixed point in the sinusoidal cycle (in a 74–79 degree window; dotted lines in Fig. 1*F*). Using this measurement, mAChR activation also increased the slope (Fig. 1*H*), and was significant when averaged over the theta range (0.031 ± 0.0031 to 0.036 ± 0.0027 V s^{-1}, $P = 0.0028$).

Muscarine increases spike presence and broadens the frequency band for 1 : 1 phase locking

An increase in AP reliability can arise from a change in AP presence and/or a change in the precision of APs. We therefore first asked whether mAChR activation induced a change in AP presence by examining the rotation number (R#), defined as the average number of APs per cycle. A plot of R# *versus* frequency for a representative cell is shown in Fig. 2*A*. At low frequencies, even though R# was as high as 10 spikes/cycle (Fig. 2*A*, inset), AP reliability was low (Fig. 1*E*), indicating that APs come at variable times during the cycle. As frequency increases and the duration of the cycle shortens, R# falls. When R# becomes 1, the R# 'phase locks' (Ascoli *et al.* 1977; Keener *et al.* 1981) across a range of frequencies (Fig. 2*A*) and reliability is highest. At higher

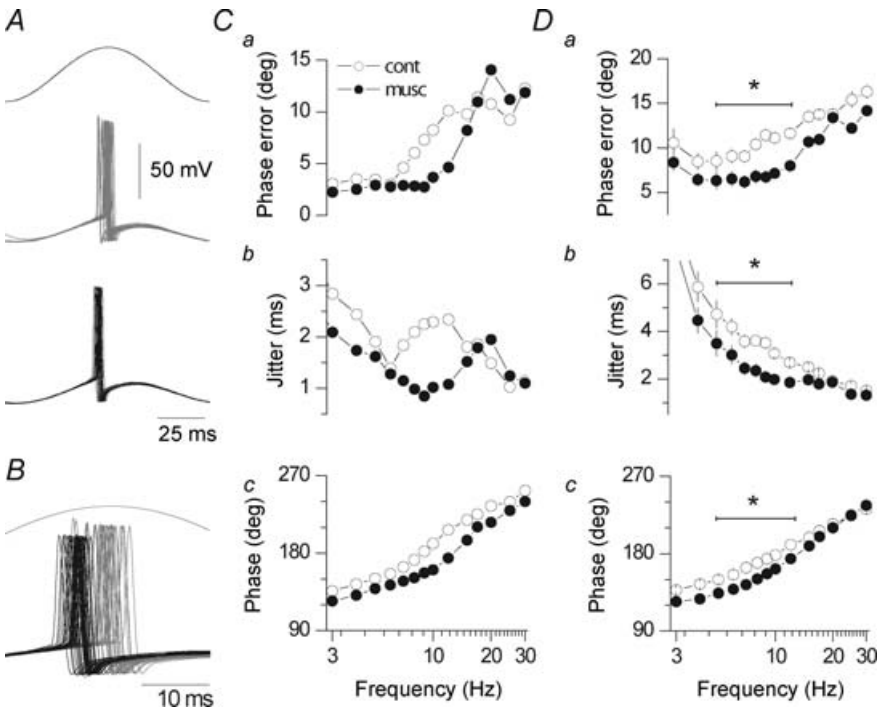

Figure 3. mAChR activation sharpens spike timing precision and induces phase shift
A and *B*, overlaying each cycle (9 Hz shown) illustrates spikes arriving earlier and more precisely in the presence of 10 μM muscarine (black traces) compared with control (grey traces). The upper trace indicates the input current over a single cycle. Changes in AP amplitude between conditions were not consistently observed. *C*, for the representative cell in *A*, plot of phase (*a*), and increase in precision, as measured in degrees (*b*) and milliseconds (*c*) *versus* frequency (○: control; ●: 10 μM muscarine). Phase was defined as the time from the trough of the input current to the time of the first spike, expressed as degrees ($t_{\text{trough-to-spike}}$ (seconds) × frequency (Hz) × 360 degrees). Precision was quantified as the standard deviation (S.D.) of the first spike time per cycle, expressed both in degrees (phase error) and seconds (jitter). *D*, in a population of 9 cells, averaging over the theta band (5–12 Hz), APs arrived significantly earlier (*a*; 170 ± 16 degrees *versus* 154 ± 12 degrees; $P = 0.03$) and more precisely (*b*, phase S.D.: 9.8 ± 1.3 degrees *versus* 6.2 ± 1.5 degrees, $P = 0.005$; *c*, jitter: 3.5 ± 0.5 ms *versus* 2.2 ± 0.6 ms, $P = 0.005$).

© 2006 The Authors. Journal compilation © 2006 The Physiological Society

frequencies, R# drops below 1 as low pass filter properties of the membrane dampen the voltage deflection. In nine cells, bath application of 10 μM muscarine caused a general increase in R# at most frequencies. This increase was statistically significant when averaged over the theta band (5–12 Hz; from 0.79 ± 0.07 to 1.11 ± 0.08, $P = 0.007$). Finally, mAChR activation broadened the plateau bandwidth (here defined as R# $= 1 \pm 0.4$) for 1 : 1 phase locking (Fig. 2*C* and *D*; 8.2 ± 2.4 Hz *versus* 15.3 ± 2.0 Hz, $n = 8$, $P < 0.02$).

mAChR activation induces phase precession and sharpens spike timing precision

To address whether mAChR activation increases AP reliability through improved spike time precision, we examined AP timing within a cycle. In an example cell, overlaying traces within a cycle (Fig. 3*A* and *B*) revealed that mAChR activation narrowed the distribution of spike times and shifted AP firing to earlier in the cycle (Fig. 3*C*). In a population of nine cells, mAChR activation improved firing precision when averaged over the theta frequency band, as measured both by phase error (Fig. 3*Da*, 9.8 ± 1.3 degrees *versus* 6.2 ± 1.5 degrees, $P = 0.005$) and spike jitter (Fig. 3*Db*, 3.5 ± 0.5 ms *versus* 2.2 ± 0.6 ms, $P = 0.005$). In addition, mAChR activation shifted spike timing to earlier in the cycle (Fig. 3*Dc*, 170 ± 16 degrees *versus* 154 ± 12 degrees; $P = 0.03$). Thus, mAChR activation increases AP reliability through improvements in both phase locking and spike timing precision in O-LM interneurones.

Finally, we determined how mAChR-induced ADPs (Lawrence *et al.* 2006) influenced oscillatory input in O-LM cells. We triggered a mAChR-induced ADP by introducing 4 s long, 5 Hz oscillatory inputs from a hyperpolarized potential of −60 mV (Fig. 4). Over the course of sinusoidal stimulation, a mAChR-induced ADP developed (Fig. 4*A*; by 1.7 ± 0.5 mV, $P = 0.01$, $n = 10$), which was accompanied by an increase in AP probability

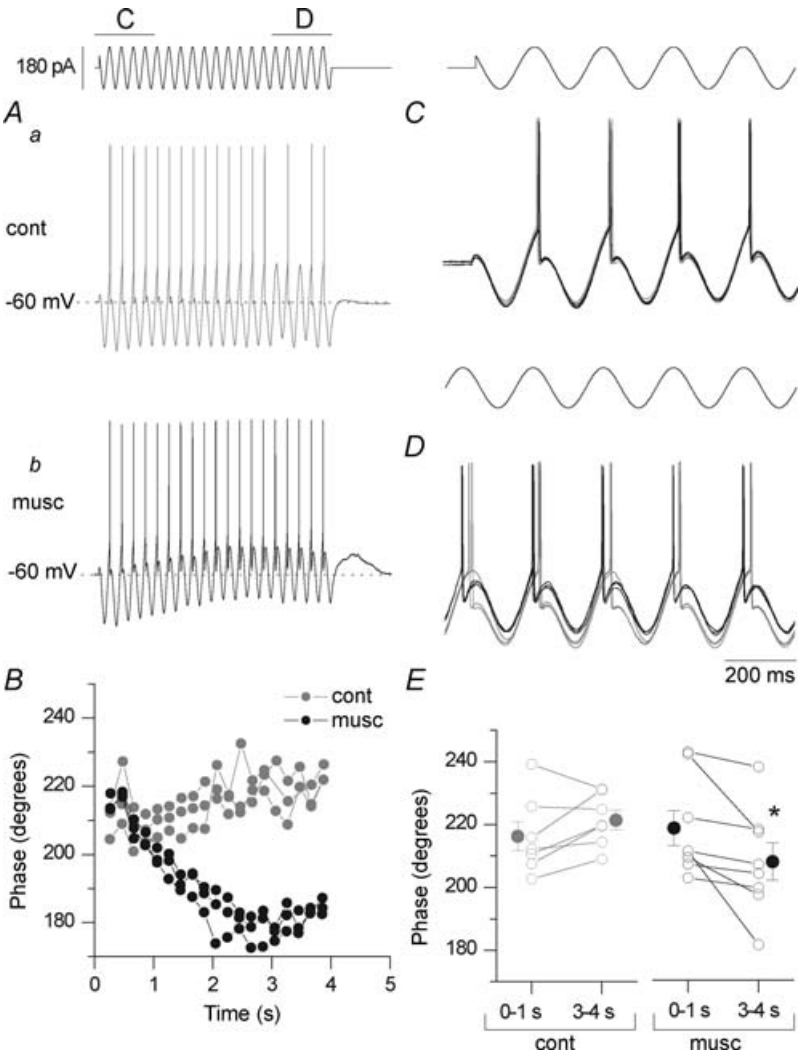

Figure 4. Muscarinic ADPs are associated with AP phase shift in O-LM interneurones
A, representative voltage output in response to a 4 s, 90 pA sinusoidal current in the absence (*a*) or presence (*b*) of 10 μM muscarine. *B*, AP phase over the course of the 4 s train for 3 trials in both control (grey) and 10 μM muscarine (black). Expanded, overlaid traces during the first (*C*; 0–1 s in *A*) or last (*D*; 3–4 s in *A*) second of the sinusoidal current injection. While the APs occur at a similar time in the cycle initially, mAChR activation shifts the timing of AP generation to earlier in the cycle. *E*, phase for control (grey; $n = 7$) and upon mAChR activation (black; $n = 8$) in the first (0–1) or last (3–4) second. In control conditions, the phase increased from 212 ± 3 to 220 ± 3 degrees (6 of 7 cells, $P = 0.03$; $P = 0.13$ for all 7 cells). Concomitant with the development of a muscarinic ADP (by 1.7 ± 0.5 mV, $P = 0.01$, $n = 10$), mAChR activation shifted phase from 218 ± 6 to 208 ± 6 degrees ($n = 8$, $P = 0.026$). The ADP was measured by comparing the difference in average voltage in seconds 0–1 *versus* 3–4 of the sinusoidal stimulation; the sinusoidal stimulation itself generated no net voltage difference in control conditions (see Methods).

© 2006 The Authors. Journal compilation © 2006 The Physiological Society

(from 0.42 ± 0.11 to 0.71 ± 0.09, $n = 10$, $P = 0.002$). In a population of cells in which phase could be measured reliably in control ($n = 7$) and muscarinic ($n = 8$) conditions, mAChR activation induced a shift in average phase (from 219 ± 4 to 206 ± 5 degrees, $n = 7$, $P = 0.006$). However, this shift in phase was progressive over the course of the sinusoidal stimulation (Fig. 4*A* and *B*); while the APs occurred at a similar time in the cycle initially (Fig. 4*C*), mAChR activation shifted the timing of AP generation to earlier in the cycle (Fig. 4*D*). Comparing the first (0–1) and last (3–4) second of the sinusoidal stimulation, phase in control conditions increased from 212 ± 3 to 220 ± 3 degrees (Fig. 4*E*, grey; 6 of 7 cells, $P = 0.03$; $P = 0.13$ for all 7 cells). Upon mAChR activation, phase shifted from 218 ± 6 degrees at seconds 0–1 to 208 ± 6 degrees at seconds 3–4 ($n = 8$, $P = 0.026$). Thus, mAChR activation can induce phase shift and an increase in AP probability in O-LM cells, which can occur through both depolarization-dependent and -independent mechanisms.

Discussion

Mechanisms underlying mAChR-induced changes in the oscillatory properties of O-LM neurones

The spike transfer frequency preference of a neurone emerges from a complex interplay between active conductances and the low-pass filtering characteristics of the cell, but it is unclear how neuromodulation impacts on these processes. We previously identified three ionic conductances that are modulated by mAChR activation in O-LM cells: an M-current (I_M), a calcium-activated potassium conductance (I_{AHP}), and a calcium-dependent cationic conductance (I_{CAT}; Lawrence *et al.* 2006). On the basis of these mAChR-dependent conductances, we propose that inhibition of I_M and I_{AHP}, coupled to the activation of I_{CAT}, increases AP reliability and spike precision during oscillatory input through the following mechanisms. mAChR modulation of these three conductances together depolarizes the cell, as revealed by an increase in holding current at -60 mV (Lawrence *et al.* 2006). In control conditions, activation of I_M, coupled to activity-dependent activation of I_{AHP}, progressively shunts and dampens oscillatory input. However, when mAChRs are activated, these forces are inhibited and I_{CAT} activated. These collective conductances essentially counteract each other such that no net change in input resistance occurs outside of the range of activation of mAChR-sensitive conductances. However, near threshold potentials, mAChR activation causes a relative increase in the input resistance, which increases the slope during the upswing of the cycle compared to control conditions (Fig. 1*F* and *G*). The increased slope effectively lowers the threshold for AP initiation (Azouz & Gray, 2000), accounting for increased AP reliability, phase locking, precision, and phase shift observed upon mAChR activation (Figs 1–3). Thus, tuning of the oscillatory properties of O-LM interneurones requires the coordinated inhibition of I_M and I_{AHP} and activation of I_{CAT} in the proximity of the activated mAChRs. Future modelling studies will likely reveal the role that each of these conductances contributes to mAChR-induced changes in spike timing and reliability.

mAChR activation tunes the intrinsic oscillatory properties of O-LM to amplify spike transmission at theta frequencies

In vivo studies have indicated that cholinergic transmission plays a key role in the amplification of theta rhythmicity (Lee *et al.* 1994). Here we show that mAChR-mediated amplification can occur postsynaptically in a specific subpopulation of hippocampal interneurone, the O-LM cells. This amplification arises from depolarization-dependent and -independent mechanisms, increasing AP reliability, precision, and 1 : 1 firing all at theta frequencies. Moreover, mAChR activation induced phase shift solely through postsynaptic means, a phenomenon that may be relevant to information coding during theta oscillations *in vivo* (Buzsaki, 2002). These changes may translate into increased synchrony in the rhythmic disinhibition of pyramidal cells, facilitating the entrainment of pyramidal cells at theta frequencies.

What is the signficance of mAChR activation of O-LM interneurones during theta oscillations? A recent model of theta oscillations, which reproduces experimentally observed phase relationships in pyramidal cells and interneurones, suggests that O-LM neurones participate in the retrieval cycle of the theta wave in which entorhinal cortical input to the hippocampus is at a minimum (Kunec *et al.* 2005). During this time, O-LM cells prevent weak afferents of the entorhinal cortex not involved in encoding the memory from reaching threshold. The model predicts that memory encoding and retrieval is best when O-LM cells discharge on every theta cycle. Thus, cholinergic input from the septum may optimize memory retrieval by promoting phase locking of O-LM cells at theta frequency.

References

Ascoli C, Barbi M, Chillemi S & Petracchi D (1977). Phase-locked responses in the *Limulus* lateral eye. Theoretical and experimental investigation. *Biophys J* **19**, 219–240.

Azouz R & Gray CM (2000). Dynamic spike threshold reveals a mechanism for synaptic coincidence detection in cortical neurons in vivo. *Proc Natl Acad Sci U S A* **97**, 8110–8115.

© 2006 The Authors. Journal compilation © 2006 The Physiological Society

Buzsaki G (2002). Theta oscillations in the hippocampus. *Neuron* **33**, 325–340.

Cobb SR, Buhl EH, Halasy K, Paulsen O & Somogyi P (1995). Synchronization of neuronal activity in hippocampus by individual GABAergic interneurons. *Nature* **378**, 75–78.

Cobb SR & Davies CH (2005). Cholinergic modulation of hippocampal cells and circuits. *J Physiol* **562**, 81–88.

Fellous JM & Sejnowski TJ (2000). Cholinergic induction of oscillations in the hippocampal slice in the slow (0.5–2 Hz), theta (5–12 Hz), and gamma (35–70 Hz) bands. *Hippocampus* **10**, 187–197.

Garcia-Munoz A, Barrio LC & Buno W (1993). Membrane potential oscillations in CA1 hippocampal pyramidal neurons in vitro: intrinsic rhythms and fluctuations entrained by sinusoidal injected current. *Exp Brain Res* **97**, 325–333.

Gloveli T, Dugladze T, Saha S, Monyer H, Heinemann U, Traub RD, Whittington MA & Buhl EH (2005). Differential involvement of oriens/pyramidale interneurones in hippocampal network oscillations in vitro. *J Physiol* **562**, 131–147.

Keener JP, Hoppensteadt FC & Rinzel J (1981). Integrate-and-fire models of nerve membrane response to oscillatory input. *Siam J Appl Math* **41**, 503–517.

Klausberger T, Magill PJ, Marton LF, Roberts JD, Cobden PM, Buzsaki G & Somogyi P (2003). Brain-state- and cell-type-specific firing of hippocampal interneurons in vivo. *Nature* **421**, 844–848.

Klausberger T, Marton LF, Baude A, Roberts JD, Magill PJ & Somogyi P (2004). Spike timing of dendrite-targeting bistratified cells during hippocampal network oscillations in vivo. *Nat Neurosci* **7**, 41–47.

Kunec S, Hasselmo M & Kopell N (2005). Encoding and retrieval in the CA3 region of the hippocampus: a model of theta phase separation. *J Neurophysiol* **94**, 70–82.

Lawrence JJ, Statland JM, Grinspan ZM & McBain CJ (2006). Cell type-specific dependence of muscarinic signaling in mouse hippocampal stratum oriens interneurons. *J Physiol* **570**, 595–610.

Lee MG, Chrobak JJ, Sik A, Wiley RG & Buzsaki G (1994). Hippocampal theta activity following selective lesion of the septal cholinergic system. *Neuroscience* **62**, 1033–1047.

Leung LS & Yu HW (1998). Theta-frequency resonance in hippocampal CA1 neurons in vitro demonstrated by sinusoidal current injection. *J Neurophysiol* **79**, 1592–1596.

Lisman JE & Idiart MA (1995). Storage of 7 +/– 2 short-term memories in oscillatory subcycles. *Science* **267**, 1512–1515.

McBain CJ, DiChiara TJ & Kauer JA (1994). Activation of metabotropic glutamate receptors differentially affects two classes of hippocampal interneurons and potentiates excitatory synaptic transmission. *J Neurosci* **14**, 4433–4445.

Maccaferri G (2005). Stratum oriens horizontal interneuron diversity and hippocampal network dynamics. *J Physiol* **562**, 73–80.

McMahon LL, Williams JH & Kauer JA (1998). Functionally distinct groups of interneurons identified during rhythmic carbachol oscillations in hippocampus in vitro. *J Neurosci* **18**, 5640–5651.

McQuiston AR & Madison DV (1999*a*). Muscarinic receptor activity has multiple effects on the resting membrane potentials of CA1 hippocampal interneurons. *J Neurosci* **19**, 5693–5702.

McQuiston AR & Madison DV (1999*b*). Muscarinic receptor activity induces an afterdepolarization in a subpopulation of hippocampal CA1 interneurons. *J Neurosci* **19**, 5703–5710.

Pike FG, Goddard RS, Suckling JM, Ganter P, Kasthuri N & Paulsen O (2000). Distinct frequency preferences of different types of rat hippocampal neurones in response to oscillatory input currents. *J Physiol* **529**, 205–213.

Reich CG, Karson MA, Karnup SV, Jones LM & Alger BE (2005). Regulation of IPSP theta rhythm by muscarinic receptors and endocannabinoids in hippocampus. *J Neurophysiol* **94**, 4290–4299.

Schreiber S, Fellous JM, Tiesinga P & Sejnowski TJ (2004). Influence of ionic conductances on spike timing reliability of cortical neurons for suprathreshold rhythmic inputs. *J Neurophysiol* **91**, 194–205.

Schreiber S, Fellous JM, Whitmer D, Tiesinga P & Sejnowski TJ (2003). A new correlation-based measure of spike timing reliability. *Neurocomputing* **52–54**, 925–931.

Somogyi P & Klausberger T (2005). Defined types of cortical interneurone structure space and spike timing in the hippocampus. *J Physiol* **562**, 9–26.

Whittington MA & Traub RD (2003). Interneuron diversity series: inhibitory interneurons and network oscillations in vitro. *Trends Neurosci* **26**, 676–682.

Acknowledgements

This work was supported by NICHD intramural and HFSP funding to C.Mc.B. We thank Brian Jeffries for immunocytochemistry and Drs Maciej Lazarewicz and Mark Stopfer for critically reading an earlier version of the manuscript. Z.M.G and J.M.S. are HHMI-NIH Research Scholars.

Supplemental material

The online version of this paper can be accessed at:
DOI: 10.1113/jphysiol.2005.103218
http://jp.physoc.org/cgi/content/full/jphysiol.2005.0103218/DC1
and contains supplemental material consisting of an Appendix and a figure entitled The reliability statistic.

This material can also be found as part of the full-text HTML version available from http://www.blackwell-synergy.com

© 2006 The Authors. Journal compilation © 2006 The Physiological Society